

GranQ: Granular Zero-Shot Quantization with Channel-Wise Activation Scaling in QAT

Inpyo Hong, Youngwan Jo, Hyojeong Lee, Sunghyun Ahn, Kijung Lee, Sanghyun Park*

Yonsei University

{hip9863, jyy1551, hyojoy, skd, rlwjd4177, sanghyun}@yonsei.ac.kr

Abstract

Zero-shot quantization (ZSQ) enables neural network compression without original training data, making it a promising solution for restricted data access scenarios. To compensate for the lack of data, recent ZSQ methods typically rely on synthetic inputs generated from the full-precision model. However, these synthetic inputs often lead to activation distortion, especially under low-bit settings. To mitigate this, existing methods typically employ per-channel scaling, but they still struggle due to the severe computational overhead during the accumulation process. To overcome this critical bottleneck, we propose *GranQ*, a novel activation quantization framework that introduces an efficient pre-scaling strategy. Unlike conventional channel-wise methods that repeatedly perform scaling operations during accumulation, *GranQ* applies scaling factors in a pre-scaling step through fully vectorized computation, eliminating runtime scaling overhead. This design enables *GranQ* to maintain fine-grained quantization accuracy while significantly reducing computational burden, particularly in low-bit quantization settings. Extensive experiments under quantization-aware training (QAT) settings demonstrate that *GranQ* consistently outperforms state-of-the-art ZSQ methods across CIFAR and ImageNet. In particular, our method achieves up to 5.45% higher accuracy in the 3-bit setting on CIFAR-100 and even surpasses the full-precision baseline on CIFAR-10. Furthermore, *GranQ* achieves significant speedup in quantization latency over conventional per-channel methods, demonstrating improved efficiency. With these findings, we anticipate that *GranQ* will inspire future research beyond conventional ZSQ approaches centered on data generation and model fine-tuning. The official code is available at <https://github.com/anonymous-orange/GranQ>.

Introduction

Neural network compression has been extensively studied for the practical deployment of large-scale deep learning (DL) models. In particular, reducing model size while minimizing performance degradation is crucial for utilizing DL on edge devices (e.g., mobile phones, embedded systems, and drones). Major approaches to model compression include quantization (Hubara et al. 2018; Li et al. 2021; Gholami et al. 2022), pruning (LeCun, Denker, and Solla 1989; Frankle and Carbin 2018; Liu et al. 2018; Cheng,

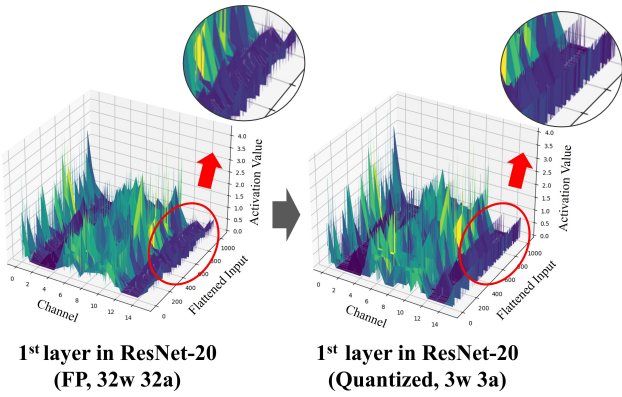
Data Generation (PTQ, QAT)	Calibration (PTQ)	Fine-tuning (QAT)
ZeroQ (<i>CVPR 20</i>)		
GDFQ (<i>ECCV 20</i>)		
DSG (<i>CVPR 21</i>)		
MixMix (<i>CVPR 21</i>)		
Qimera (<i>NeurIPS 21</i>)		AIT (<i>CVPR 22</i>)
IntraQ (<i>CVPR 22</i>)	SQuant (<i>ICLR 22</i>)	PLF (<i>CVPR 24</i>)
GENIE (<i>CVPR 23</i>)	UDFC (<i>ICCV 23</i>)	SynQ (<i>ICLR 25</i>)
AdaDFQ (<i>CVPR 23</i>)		GranQ (<i>Ours</i>)
Casual-DFQ (<i>ICCV 23</i>)		
TexQ (<i>NeurIPS 23</i>)		
RIS (<i>AAAI 24</i>)		
GenQ (<i>ECCV 24</i>)		

Table 1: Categorizing ZSQ algorithms. PTQ denotes post-training quantization, and QAT denotes quantization-aware training. Data generation methods typically support both PTQ and QAT, whereas **violet-marked methods** utilize fine-tuning for data generation and **support only QAT**.

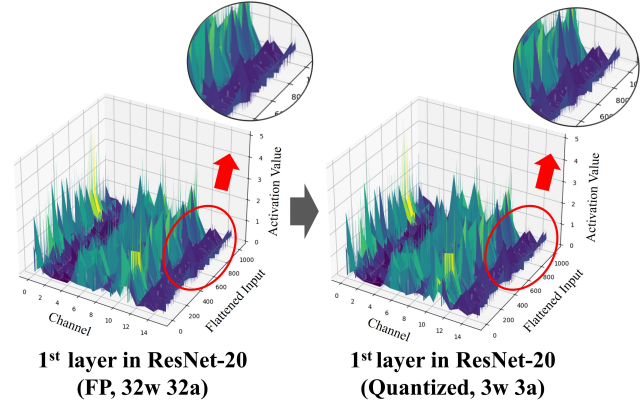
Zhang, and Shi 2024), knowledge distillation (Hinton 2015; Heo et al. 2019; Wang and Yoon 2021), and neural architecture search (Zoph 2016; Elsken, Metzen, and Hutter 2019), as surveyed in (Cheng et al. 2018; Deng et al. 2020). Among these, quantization has emerged as the most actively studied technique. It serves as an effective compression method by reducing unnecessary representational ranges in the model. However, it often requires fine-tuning or calibration to match full-precision (FP) model performance (Gholami et al. 2022). To address this, zero-shot quantization (ZSQ), also known as data-free quantization, has been proposed to compress models without the original training data.

Since the introduction of ZeroQ (Cai et al. 2020), studies on ZSQ have advanced in two main directions. The first direction focuses on data generation, where synthetic data are created from the FP model. The second direction focuses on effectively applying the activation distributions of the synthetic data to the quantized (Q) model. This second direction is further divided into post-training quantization (PTQ), which calibrates the activation distributions, and quantization-aware training (QAT), which fine-tunes the Q model directly. We categorize existing ZSQ methods based on these directions, as summarized in Table 1.

*Corresponding Author



(a) Layer-wise Quantization



(b) *GranQ* (Channel-wise, Ours)

Figure 1: Comparison between (a) layer-wise quantization and (b) *GranQ* on the CIFAR-10. Each subfigure visualizes the 32-bit FP (left) and 3-bit quantized (right) activations of the first ResNet-20 layer. *GranQ* better preserves the original activation with minimal distortion.

First, data generation studies focus on generating high-quality data to effectively train the Q model (Xu et al. 2020; Qian et al. 2023; Li et al. 2024). Meanwhile, calibration (PTQ) studies aim to minimize the quantization error by calibrating the Q model without additional training (Guo et al. 2022; Bai et al. 2023). Finally, fine-tuning (QAT) studies focus on transferring key information from the FP model to the Q model through knowledge distillation (Choi et al. 2022; Fan et al. 2024; Hong et al. 2025; Kim, Kim, and Kang 2025).

However, despite extensive studies, severe performance degradation in low-bit quantization remains unresolved. To address this issue, we performed an in-depth analysis of the ZSQ process, focusing on why low-bitwidth settings still suffer from performance loss even after QAT fine-tuning. Our findings reveal that quantization errors mainly stem from the loss of activation values instead of data quality or training methods. Notably, we found that layer-wise (per-tensor) quantization is no longer suitable for preserving activations in ZSQ, as it leads to coarse and inaccurate representations.

Based on this analysis, we introduce *GranQ*, a novel ZSQ method that achieves efficient per-channel quantization via vectorized pre-scaling of input-dependent activations. This dynamic adjustment minimizes activation loss and preserves the original activation values by reducing quantization errors, as shown in Figure 1. The proposed method effectively handles activation loss in low-bit quantization and achieves state-of-the-art (SOTA) performance in QAT settings on the CIFAR and ImageNet datasets. Furthermore, we apply vectorization to the pre-scaling step, which is typically omitted in conventional channel-wise quantization, thereby reducing latency and enabling fine-grained activation quantization. Our contributions can be summarized as follows:

- **We identify critical limitations of layer-wise activation quantization in low-bit ZSQ.** Our findings reveal that conventional activation quantization methods relying on layer-wise granularity suffer from significant acti-

vation loss. This limitation becomes more severe in ZSQ settings with synthetic data.

- **We propose *GranQ*, a novel method that supports granular quantization and maintains computational efficiency.** Although per-channel activation quantization is known to improve precision, it has not been widely adopted due to its high computational cost. We address this by introducing vectorized pre-scaling, which integrates per-channel scaling into the quantization step, allowing accumulation to proceed efficiently without runtime scaling overhead. To the best of our knowledge, our approach is the first to address the ZSQ problem.
- **We achieve SOTA performance over existing ZSQ methods through extensive evaluation.** Specifically, on the CIFAR-100 dataset, in the 3-bit quantization setting, *GranQ* achieves an accuracy of 62.73%, improving by 5.45% over the latest method on ResNet-20. Furthermore, on the CIFAR-10 dataset in the 5-bit quantization setting, *GranQ* achieves an accuracy of 94.06%, slightly exceeding the FP model performance by 0.17%.

Related Work

Quantization

Quantization reduces the representational range of deep neural networks (DNNs) and minimizes memory usage. It is typically categorized into post-training quantization (PTQ) and quantization-aware training (QAT) (Gholami et al. 2022; Banner, Nahshan, and Soudry 2019). PTQ applies quantization after training without further updates, which makes it efficient and easy to implement. However, it is sensitive to scaling errors and often relies on calibration to improve accuracy. In contrast, QAT incorporates quantization during training and optimizes quantized activations using the straight-through estimator (Gholami et al. 2022; Yin et al. 2019). Both methods require data. PTQ uses it for calibration, while QAT uses it for fine-tuning.. In practice, access to training data is often limited. To address this, zero-shot

quantization (ZSQ) has been proposed to perform quantization without using original data (Xu et al. 2020).

Zero-shot Quantization

As summarized in Table 1, ZSQ was initially introduced by ZeroQ (Cai et al. 2020), leading to the development of various ZSQ algorithms. These studies have explored diverse approaches to improve quantization performance under data-free settings. Recent studies have focused on generating high-quality synthetic data (Jeon, Lee, and Kim 2023; Li et al. 2024) and developing more effective methods to utilize them (Choi et al. 2022; Hong et al. 2025; Kim, Kim, and Kang 2025). However, current ZSQ methods heavily rely on augmented synthetic inputs. This causes large variation in activation scales across channels. In practice, such input-dependent channel-wise quantization is rarely adopted due to its high computational cost. Therefore, recent studies have applied channel-wise activation quantization either in a limited conditions within QAT settings (Cho and Yoo 2020), or exclusively in PTQ scenarios with access to a small amount of data (Yvinec et al. 2023; Xu et al. 2024). This highlights the importance of efficient channel-wise activation quantization in QAT.

Preliminaries and Problem Definition

In this section, we provide a new definition of the existing ZSQ problem and introduce the preliminaries. The detailed mathematical notations are listed in Table 6 in the appendix.

Activation Quantization

Activation quantization reduces the precision of intermediate activation values by converting them into low-bitwidth integers (Choi et al. 2018). It is commonly used with weight quantization to compress models, and the linear quantization scheme is most widely adopted. This process typically consists of quantization, scaling parameter computation, and dequantization (Hubara et al. 2018; Gholami et al. 2022; Fang et al. 2020).

The quantization operator Q maps a floating-point value x into an integer x_q using a scaling factor s and zero-point z :

$$x_q = Q(x, s, z) = \left\lfloor \frac{x}{s} + z \right\rfloor \quad (1)$$

Here, s normalizes the activation range, and z shifts the scaled value to account for asymmetric quantization. These parameters are computed as:

$$s = \frac{x_{\max} - x_{\min}}{2^b - 1}, \quad z = \left\lfloor \frac{-x_{\min}}{s} \right\rfloor \quad (2)$$

where x_{\min} and x_{\max} denote the range of activation values, and b is the bit-width. A large range yields a large s , increasing quantization error, a smaller range allows finer resolution. As shown below, in quantized models, per-channel scaling is embedded directly into the accumulation path, requiring each channel to be individually scaled during computation:

$$y_l = \sum_{c=1}^C w_c \cdot s_c \cdot (x_{q,c} - z_c) \quad (3)$$

However, applying the per-channel scaling factor s_c inside the accumulation loop introduces computational overhead, making efficient integer-domain execution difficult. This scaling bottleneck hinders parallelism in core operations such as convolution and matrix multiplication, reducing the efficiency of quantized models (Nagel et al. 2021).

Problem Definition

Existing activation quantization methods are designed based on layer-wise quantization to minimize computational cost. However, a fixed scaling factor struggles to handle varying activations. This issue becomes more severe under low-bitwidth settings in ZSQ environments. The following outlines the primary challenges faced in ZSQ under low-bitwidth settings.

(Problem 1) Coarse Activation Quantization by Single-Range Scaling

Conventional activation quantization uses a single scaling range per layer for efficiency, which was acceptable at higher bitwidths or when real data is available. However, this design becomes problematic in ZSQ, where range adjustment relies on synthetic data. These synthetic distributions are often biased or irregular, making precise quantization more difficult.

(Problem 2) Accumulation Bottleneck in Channel-wise Quantization

The main challenge in channel-wise quantization lies not in quantizing activations but in the repeated per-channel scaling during accumulation. This disrupts vectorized execution and significantly increases computational overhead.

Observation and Methodology

We observe the causes of activation distortion during quantization and analyze how to mitigate them. Based on this, we introduce our method, *GranQ*.

Observation

Layer-wise quantization effectively captures the activation distribution of each layer. However, it becomes inefficient when activation distributions within a layer exhibit significant variation along the channel axis. Particularly in ZSQ, as shown in the activation magnitudes in Appendix Figure 6, the activation distributions can differ substantially across layers. This implies that limited representation bits are forced to capture a wide range of activation values, making fine-grained quantization difficult. It consistently appears across all layers. We analyzed this phenomenon occurring across all layers and provided a summary in Table 2.

Activation Quantization	Layer-wise	Channel-wise (<i>GranQ</i>)
Avg. $\frac{\ X \cdot Q\ _2}{\ X\ _2 \ Q\ _2} (\uparrow)$	0.5111	0.6835
Avg. $\frac{\ X - Q\ _2}{\ X\ _2} (\downarrow)$	0.3129	0.1063

Table 2: Average cosine similarity and relative error for 3-bit activation quantization on ResNet-20 (CIFAR-100). *GranQ* shows lower activation distortion than layer-wise, with higher similarity and lower error.

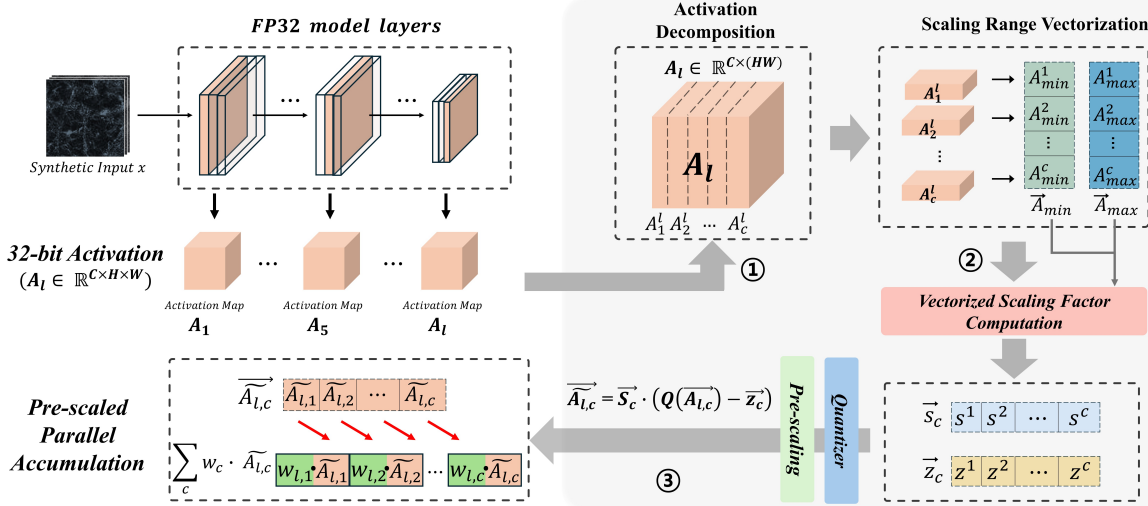


Figure 2: Overview of the *GranQ* algorithm. ① Each activation map A_l is decomposed into channel-wise vectors (see Equation 4). ② Min/max values are extracted per channel to compute scaling factors and zero-points in a vectorized form.(see Equations 5). ③ $\vec{A}_{l,c}$ is quantized as $Q(\vec{A}_{l,c})$, and the scaling factor \vec{s}_c is applied in advance to enable pre-scaled parallel accumulation (see Equation 6).

It presents the cosine similarity $\frac{X \cdot Q}{|X|_2 |Q|_2}$, along with the relative error $\frac{|X - Q|_2}{|X|_2}$. From the results, we observe that layer-wise quantization fails to preserve activation information effectively. **This reveals that using a single scaling range for activation quantization has a critical limitation, particularly in ZSQ.** In contrast, *GranQ*, which applies scaling per channel, achieves $1.34\times$ higher similarity and $2.94\times$ lower relative error than layer-wise quantization, demonstrating its effectiveness in preserving activation information.

Furthermore, Figure 1a illustrates how layer-wise quantization leads to coarse activation representations across layers. Fine-grained activation values are often mapped to limited discrete levels, resulting in a loss of detail and reduced representational capacity. This degradation contributes to decreased inference performance.

Methodology

Based on our analysis, we propose *GranQ*, a fine-grained ZSQ method designed to reduce computational overhead, as illustrated in Figure 2. *GranQ* applies channel-wise scaling through *activation decomposition*, and achieves fast parallel processing via *pre-scaling for parallel accumulation*, which enables efficient computation of both scaling and quantization.

Activation Decomposition We propose *activation decomposition*, which reshapes each activation map from a three-dimensional tensor of shape $(C \times H \times W)$ into a two-dimensional matrix of shape $(C \times HW)$. This transformation enables decomposition of the activation map along the channel axis, allowing each channel to be processed independently. It also facilitates vectorized computation of per-channel statistics (e.g., min and max) required for scaling

Algorithm 1: *GranQ*: Pre-scaling for Parallel Accumulation

Require: Activation tensors $\{A_l\}_{l=1}^L$, where $A_l \in \mathbb{R}^{C \times H \times W}$, quantization bit b , weight tensors $\{w_{l,c}\}_{l=1, c=1}^{L, C}$

Ensure: Output vectors $\{y_l\}_{l=1}^L$

- 1: **for** each layer l in L **do**
- 2: $A_l \leftarrow \text{reshape}(A_l) \in \mathbb{R}^{C \times (HW)}$
- 3: $\vec{A}_{\min}, \vec{A}_{\max} \leftarrow \min_{h,w}(A_l), \max_{h,w}(A_l)$
- 4: $\vec{s}_l \leftarrow (\vec{A}_{\max} - \vec{A}_{\min}) / (2^b - 1)$
- 5: $\vec{z}_l \leftarrow \lfloor -\vec{A}_{\min} / \vec{s}_l \rfloor$
- 6: $\vec{A}_{q,l} \leftarrow \lfloor A_l / \vec{s}_l + \vec{z}_l \rfloor$ ▷ quantize (int mapping)
- 7: $\vec{A}_{l,c} \leftarrow \vec{s}_l \cdot (\vec{A}_{q,l} - \vec{z}_l)$ ▷ dequantize & pre-scale
- 8: **Compute output:**

$$y_l = \sum_{c=1}^C w_{l,c} \cdot \vec{A}_{l,c}$$

9: **end for**
10: **return** $\{y_l\}_{l=1}^L$

factor calculation during quantization. We define the *activation decomposition* as shown in Equation 4.

$$A_l = [A_l(1, :, :), A_l(2, :, :), \dots, A_l(C, :, :)] \in \mathbb{R}^{C \times H \times W}$$

$$\vec{A}_{\min} = \left[\min_{(h,w)} A_l(c, h, w) \right]_{c=1}^C \in \mathbb{R}^C$$

$$\vec{A}_{\max} = \left[\max_{(h,w)} A_l(c, h, w) \right]_{c=1}^C \in \mathbb{R}^C$$
(4)

Here, the vectors \vec{A}_{\min} and \vec{A}_{\max} denote the channel-wise minimum and maximum values computed from the activa-

tion input A_l of each layer, where $A_l \in \mathbb{R}^{C \times H \times W}$. Unlike traditional layer-wise quantization that applies a single scalar across all channels, this representation allows for independent normalization of each channel. As part of the *activation decomposition* stage (see ① in Figure 2), the activation tensor is spatially flattened and separated by channel to enable the computation of per-channel scaling factors. Algorithm 2 in the appendix clearly illustrates the difference between our method (Algorithm 1) and conventional channel-wise quantization.

Pre-scaling for Parallel Accumulation

$$\vec{s} = \frac{\vec{A}_{\max} - \vec{A}_{\min}}{2^b - 1}, \quad \vec{z} = \left\lfloor -\frac{\vec{A}_{\min}}{\vec{s}} \right\rfloor \quad (5)$$

$$y_l = \sum_{c=1}^C w_{l,c} \cdot \vec{A}_{l,c}, \quad \text{where } \vec{A}_{l,c} = \vec{s}_c \cdot \left(\left\lfloor \frac{\vec{A}_{l,c}}{\vec{s}_c} + \vec{z}_c \right\rfloor - \vec{z}_c \right) \quad (6)$$

In the *pre-scaling for parallel accumulation* stage, the scaling factors \vec{s}_c and zero-points \vec{z}_c are computed in a vectorized form across channels to dynamically adapt to the diverse activation distributions induced by synthetic inputs. This contrasts with conventional per-channel quantization, which applies fixed scaling parameters per channel regardless of input variation.

As shown in Equation 6, each activation $\vec{A}_{l,c}$ is first quantized using its corresponding vectorized scaling and zero-point, and then dequantized to reconstruct the floating-point value. The resulting $\vec{A}_{l,c}$ represents a pre-scaled activation that is already adjusted for accumulation. By applying vectorized scaling, quantization, and dequantization uniformly across channels, this process enables efficient integer-domain computation and parallel accumulation with weights $w_{l,c}$.

Experiments

In this section, we thoroughly evaluate the effectiveness of GranQ. Experiments are conducted on diverse benchmark datasets, with the performance compared with those of existing ZSQ methods.

Experimental Setup and Details

The experiments were conducted using widely adopted ZSQ evaluation datasets, including CIFAR-10, CIFAR-100 (Krizhevsky, Hinton et al. 2009), and ImageNet (ILSVRC 2012) (Deng et al. 2009) validation datasets. For the CIFAR datasets, ResNet-20 (He et al. 2016) was used as the quantization model, whereas ResNet-18 (He et al. 2016), ResNet-50 (He et al. 2016), and MobileNetV2 (Sandler et al. 2018) were employed for ImageNet. All experiments were conducted using the SGD optimizer (Ruder 2016) with a momentum of 0.9 and weight decay of 1e-4. The CIFAR-10 and CIFAR-100 experiments were each conducted for 200 epochs, with batch sizes of 16 and 200, respectively. For ImageNet, we trained for 400 epochs with a batch size of 16. The initial learning rate was set to 1e-4 for CIFAR-10 and

CIFAR-100, and 1e-5 for ImageNet, with multi-step learning rate decay applied. The decay steps were set to 100, 200, and 300 epochs for CIFAR, and at 350 and 400 epochs for ImageNet, with a decay rate of 0.1. We compared our method with existing ZSQ methods (Xu et al. 2020; Choi et al. 2022; Qian et al. 2023; Chen et al. 2024; Bai et al. 2024; Fan et al. 2024; Li et al. 2024; Hong et al. 2025; Kim, Kim, and Kang 2025). For data generation, we followed the AdaDFQ (Qian et al. 2023) approach based on ACGAN (Odena, Olah, and Shlens 2017). Further implementation details are provided in the appendix, Section and . In our ablation study, layer-wise quantization was applied to all layers containing activation functions, while channel-wise quantization was performed per channel at the batch level.

Performance Evaluation

We evaluated the performance of *GranQ* against SOTA ZSQ methods, with results summarized in Table 3. All comparison experiments were conducted under 3, 4, and 5-bit quantization settings.

CIFAR-10/100. As indicated in Table 3, *GranQ* consistently achieved the highest accuracy across all bitwidths. For CIFAR-10, it attained accuracies of 94.06% (5-bit), 93.52% (4-bit), and 91.37% (3-bit). For CIFAR-100, the results were 70.05% (5-bit), 68.79% (4-bit), and 62.73% (3-bit). Notably, *GranQ* outperformed SynQ (Kim, Kim, and Kang 2025), the previous SOTA, by +5.45% in the CIFAR-100 3-bit setting. This result demonstrates its ability to effectively overcome the limitations of conventional low-bitwidth quantization techniques. Overall, *GranQ* consistently outperformed existing methods across all bitwidths in both CIFAR-10 and CIFAR-100, with particularly strong improvements in the 3-bit quantization setting. Remarkably, in the CIFAR-10 5-bit setting, *GranQ* even surpassed the performance of the FP model. These results suggest that we can effectively apply *GranQ* to small- and medium-scale datasets.

ImageNet. In the ImageNet experiments, *GranQ* achieved competitive performance across various bitwidths. Specifically, for ResNet-18, it attained top accuracies of 70.39% (4-bit) and 71.31% (5-bit). For ResNet-50, it achieved the highest accuracies of 76.63% (4-bit) and 71.31% (5-bit). Additionally, in the MobileNetV2 setting, *GranQ* achieved SOTA performance across all bitwidths (3, 4, and 5-bit). In the 3-bit setting, *GranQ* achieved the second-best accuracies, with 64.41% on ResNet-18 and 70.76% on ResNet-50. These results are -3.77% and -3.23% lower than those of GenQ, respectively. However, GenQ uses a pre-trained diffusion model (Ho, Jain, and Abbeel 2020) and prompts during data generation, leading to slower speeds compared with those of typical GAN-based methods (Xu et al. 2020). In contrast, *GranQ* enhances the quantization mechanism without heavily relying on diffusion-based data generation, as GenQ does. Although GenQ demonstrates strong performance, its code is not publicly available, and thus we could not include it in our experiments. Nevertheless, since our method is compatible with existing QAT frameworks, it could potentially benefit from GenQ’s data generation if integration becomes

Dataset	Model (FP 32)	Bits	GDFQ (ECCV 20)	ARC+AIT (CVPR 22)	AdaDFQ (CVPR 23)	TexQ (NeurIPS 24)	AIT+RIS (AAAI 24)	GenQ (ECCV 24)	AKT (SAC 25)	SynQ (ICLR 25)	GranQ (Ours)
Cifar-10	ResNet-20 (93.89)	3w3a	75.11	-	84.89	86.47	-	-	86.76	<u>88.11</u>	91.37
		4w4a	90.25	90.49	92.31	92.68	92.59	-	92.64	<u>92.76</u>	93.52
		5w5a	93.38	92.98	93.81	-	93.59	-	<u>93.83</u>	-	94.06
Cifar-100	ResNet-20 (70.33)	3w3a	47.61	-	52.74	55.87	-	-	54.68	<u>57.28</u>	62.73
		4w4a	63.39	61.05	66.81	67.18	65.99	-	66.94	<u>67.34</u>	68.79
		5w5a	66.12	68.40	<u>69.93</u>	-	69.55	-	69.75	-	70.05
ImageNet	ResNet-18 (71.47)	3w3a	20.23	-	38.10	50.28	-	68.18	49.88 [†]	52.02	<u>64.41</u>
		4w4a	60.60	65.73	66.53	67.73	67.55	<u>70.03</u>	65.89 [†]	67.90	70.39
		5w5a	68.49	70.28	70.29	-	<u>70.59</u>	-	69.40 [†]	-	71.31
	MobileNetV2 (73.03)	3w3a	1.46	-	28.99	32.80	-	<u>59.15</u>	30.56 [†]	34.21	62.42
		4w4a	59.43	66.47	65.41	67.07	-	<u>69.65</u>	64.85 [†]	67.27	70.62
		5w5a	68.11	<u>71.96</u>	71.61	-	-	-	71.71 [†]	-	72.49
	ResNet-50 (77.73)	3w3a	0.31	-	17.63	25.27	-	73.99	24.50 [†]	26.89	<u>70.76</u>
		4w4a	54.16	68.27	68.38	70.72	71.54	<u>76.10</u>	68.75 [†]	71.05	76.63
		5w5a	71.63	76.00	76.03	-	<u>76.36</u>	-	75.90 [†]	-	77.58

Table 3: Accuracy Evaluation of QAT Methods for ZSQ. w and a represent weight and activation, respectively. **Bold** values indicate the best accuracy, and underlined values denote the second-best accuracy. \dagger indicates our re-implementation with the official code.

CIFAR-100	ResNet-20 (70.33%)										
	Method	GDFQ		Qimera+AIT		AdaDFQ		AdaDFQ+AKT		Baseline	+GranQ
		Baseline	+GranQ	Baseline	+GranQ	Baseline	+GranQ	Baseline	+GranQ		
3w3a	47.61	<u>59.04^{+11.43}</u>	45.70 [†]	60.42 ^{+14.72}	52.74	<u>62.73^{+9.99}</u>	54.68	<u>62.01^{+7.33}</u>	69.75	70.21 ^{+0.46}	62.01 ^{+7.33}
4w4a	63.39	<u>66.97^{+3.58}</u>	65.80	<u>68.08^{+2.28}</u>	66.81	<u>68.79^{+1.98}</u>	66.94	<u>68.77^{+1.83}</u>	-	-	68.77 ^{+1.83}
5w5a	66.12	<u>68.96^{+2.84}</u>	69.26	<u>70.14^{+0.88}</u>	69.93	<u>70.05^{+0.12}</u>	69.75	-	-	-	70.21 ^{+0.46}

Table 4: Accuracy of existing SOTA methods with the integration of *GranQ*. GDFQ and AdaDFQ focus on data generation, whereas Qimera+AIT and AdaDFQ+AKT primarily enhance quantized model training.

possible.

Ablation Study

Effectiveness Evaluation *GranQ* consistently demonstrates performance improvements when applied to various ZSQ methods. As summarized in Table 4, *GranQ* achieves steady performance improvements when integrated with existing SOTA ZSQ techniques.

First, we analyzed the impact of *GranQ* on data synthesis-based quantization methods, specifically GDFQ (Xu et al. 2020) and AdaDFQ (Qian et al. 2023). The integration of *GranQ* into GDFQ (Xu et al. 2020) led to a notable improvement, with accuracy rising from 47.61% to 59.04% (+11.43%) in the 3-bit setting and from 63.39% to 66.97% (+3.58%) in the 4-bit setting. Similarly, AdaDFQ (Qian et al. 2023) exhibited improvements of +9.99% in the 3-bit setting (from 52.74% to 62.73%) and +1.98% in the 4-bit setting (from 66.81% to 68.79%). These results suggest that *GranQ* effectively reduces quantization errors when combined with data synthesis-based quantization methods, leading to enhanced model performance.

Furthermore, *GranQ* also exhibits significant improvements in methods focused on training quantized models,

such as Qimera+AIT (Choi et al. 2022) and AdaDFQ+AKT (Hong et al. 2025). For Qimera+AIT (Choi et al. 2022), the 3-bit accuracy increased from 45.70% to 60.42% (+14.72%). Similarly, for AdaDFQ+AKT (Hong et al. 2025), the accuracy improved from 54.68% to 62.01% (+7.33%). These findings demonstrate that *GranQ* is not only effective in data synthesis-based methods but also enhances performance during the model training process.

Efficiency Evaluation While fine-grained activation quantization often incurs high computational cost due to per-channel scaling, *GranQ* maintains efficiency by vectorizing the scaling computation. By reshaping activation tensors, our method eliminates the overhead of iterative channel-wise operations. To assess this in practice, we measured quantization latency across various batch sizes (16, 32, 64, 128, and 200). Figure 3 compares three methods: layer-wise quantization, channel-wise quantization with scalar-loop scaling (Algorithm 2 in appendix), and our method (*GranQ*), which efficiently parallelizes scaling across channels.

The two channel-wise methods perform per-channel quantization. The conventional method computes scaling factors sequentially, whereas *GranQ* pre-applies them in a

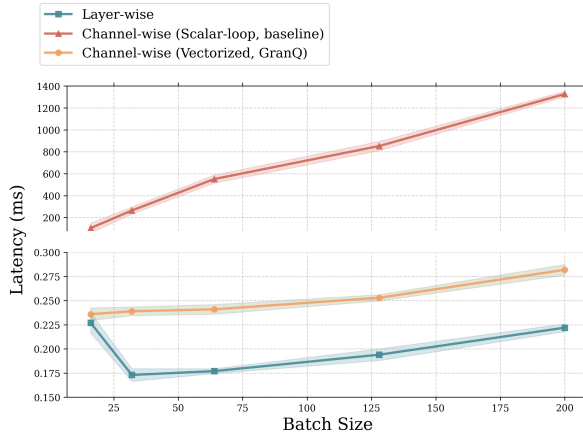


Figure 3: Latency of ResNet-20 quantization across batch sizes on CIFAR-100 with 3-bit setting.

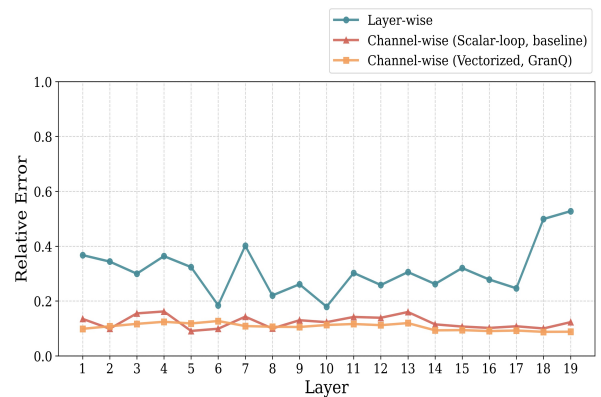


Figure 4: Relative quantization error across layers in ResNet-20 with 3-bit quantization on CIFAR-100.

Method	Quantization	Pre-Scaling	Accuracy (%)	Quantization Latency (ms)	Training Time (sec/epoch)
Layer-wise	✓		49.98	0.227	10.92
Channel-wise (Baseline)	✓		62.68	103.671	17370.54
Channel-wise (<i>GranQ</i>)	✓	✓	62.73	0.236	12.43

Table 5: Ablation study on the impact of pre-scaling and vectorization in quantization. ✓ indicates whether vectorization is applied. Latency is measured with a batch size of 16 using AdaDFQ on ResNet-20 (CIFAR-100, 3-bit).

vectorized manner across channels, enabling pre-scaling for efficient parallel accumulation. A key observation from Figure 3 is that *GranQ* achieves substantial accuracy improvement with only a minimal latency overhead compared to conventional layer-wise quantization. Furthermore, Table 2 and Figure 4 shows that *GranQ* substantially reduces quantization error and more effectively preserves activation information. These results demonstrate that *GranQ* enables fine-grained quantization with significantly improved efficiency.

Additionally, *GranQ* demonstrates that per-channel quantization can be efficiently executed by vectorizing scaling factor computation. As shown in Table 5, it achieves a quantization latency of 0.236 ms, comparable to the layer-wise baseline (0.227 ms), and significantly outperforms the conventional channel-wise method (103.671 ms) suffering from scalar-loop overhead.

Discussion

Why *GranQ* is Effective?

In layer-wise quantization, representing the entire activation range with a single scaling factor makes it difficult to reflect fine-grained distribution changes. These limitations become more severe in low-bit settings, especially when synthetic data exhibit distributional shifts. To overcome these issues, *GranQ* pre-computes per-channel scaling in a vectorized form, enabling efficient parallel accumulation. By integrating scaling into the quantization phase, we removed runtime scaling during accumulation, allowing precise and efficient parallel execution.

Limitation and Future-work

In ZSQ, synthetic data often exhibit broader and noisier activation distributions (see Figure 6 in appendix). While *GranQ* effectively handles this in QAT through dynamic per-channel scaling, its static form is less suited for PTQ. Future work will explore adapting *GranQ* to better support PTQ.

Conclusion

Layer-wise and channel-wise quantization are both commonly used in weight quantization, as weights remain fixed after training. In contrast, it is harder to apply channel-wise activation quantization because input-dependent activations make fine-grained scaling difficult. These issues are especially critical in ZSQ, with data synthesized from FP statistics. In such scenarios, synthetic activations often deviate from real data, amplifying quantization error and complicating accurate scaling. In addition, channel-wise quantization poses a computational burden due to the need for per-channel scaling during accumulation. Since scaling factors differ across channels, accumulation requires separate multiplications, limiting parallelism and increasing latency. This overhead discourages the use of channel-wise methods in practice, despite their higher representational fidelity. To address these issues, we propose *GranQ*, which vectorizes scaling to enable fine-grained quantization and efficient accumulation across channels. Through extensive experiments, we demonstrate that *GranQ* achieves notable accuracy and efficiency. Our study highlights the importance of activation preservation in ZSQ and proposes *GranQ* as an insightful direction to address this challenge.

References

Bai, J.; Yang, Y.; Chu, H.; Wang, H.; Liu, Z.; Chen, R.; He, X.; Mu, L.; Cai, C.; and Hu, H. 2024. Robustness-Guided Image Synthesis for Data-Free Quantization. In *Proceedings of the AAAI Conference on Artificial Intelligence*, volume 38, 10971–10979.

Bai, S.; Chen, J.; Shen, X.; Qian, Y.; and Liu, Y. 2023. Unified data-free compression: Pruning and quantization without fine-tuning. In *Proceedings of the IEEE/CVF International Conference on Computer Vision*, 5876–5885.

Banner, R.; Nahshan, Y.; and Soudry, D. 2019. Post training 4-bit quantization of convolutional networks for rapid-deployment. *Advances in Neural Information Processing Systems*, 32.

Cai, Y.; Yao, Z.; Dong, Z.; Gholami, A.; Mahoney, M. W.; and Keutzer, K. 2020. Zeroq: A novel zero shot quantization framework. In *Proceedings of the IEEE/CVF conference on computer vision and pattern recognition*, 13169–13178.

Chen, X.; Wang, Y.; Yan, R.; Liu, Y.; Guan, T.; and He, Y. 2024. TexQ: zero-shot network quantization with texture feature distribution calibration. *Advances in Neural Information Processing Systems*, 36.

Cheng, H.; Zhang, M.; and Shi, J. Q. 2024. A survey on deep neural network pruning: Taxonomy, comparison, analysis, and recommendations. *IEEE Transactions on Pattern Analysis and Machine Intelligence*.

Cheng, Y.; Wang, D.; Zhou, P.; and Zhang, T. 2018. Model compression and acceleration for deep neural networks: The principles, progress, and challenges. *IEEE Signal Processing Magazine*, 35(1): 126–136.

Cho, S.; and Yoo, S. 2020. Per-channel quantization level allocation for quantizing convolutional neural networks. In *2020 IEEE International Conference on Consumer Electronics-Asia (ICCE-Asia)*, 1–3. IEEE.

Choi, J.; Wang, Z.; Venkataramani, S.; Chuang, P. I.-J.; Srinivasan, V.; and Gopalakrishnan, K. 2018. Pact: Parameterized clipping activation for quantized neural networks. *arXiv preprint arXiv:1805.06085*.

Choi, K.; Lee, H. Y.; Hong, D.; Yu, J.; Park, N.; Kim, Y.; and Lee, J. 2022. It’s all in the teacher: Zero-shot quantization brought closer to the teacher. In *Proceedings of the IEEE/CVF Conference on Computer Vision and Pattern Recognition*, 8311–8321.

Deng, J.; Dong, W.; Socher, R.; Li, L.-J.; Li, K.; and Fei-Fei, L. 2009. Imagenet: A large-scale hierarchical image database. In *2009 IEEE conference on computer vision and pattern recognition*, 248–255. Ieee.

Deng, L.; Li, G.; Han, S.; Shi, L.; and Xie, Y. 2020. Model compression and hardware acceleration for neural networks: A comprehensive survey. *Proceedings of the IEEE*, 108(4): 485–532.

Elsken, T.; Metzen, J. H.; and Hutter, F. 2019. Neural architecture search: A survey. *Journal of Machine Learning Research*, 20(55): 1–21.

Fan, C.; Wang, Z.; Guo, D.; and Wang, M. 2024. Data-Free Quantization via Pseudo-label Filtering. In *Proceedings of the IEEE/CVF Conference on Computer Vision and Pattern Recognition*, 5589–5598.

Fang, J.; Shafiee, A.; Abdel-Aziz, H.; Thorsley, D.; Georgiadis, G.; and Hassoun, J. H. 2020. Post-training piecewise linear quantization for deep neural networks. In *Computer Vision–ECCV 2020: 16th European Conference, Glasgow, UK, August 23–28, 2020, Proceedings, Part II 16*, 69–86. Springer.

Frankle, J.; and Carbin, M. 2018. The lottery ticket hypothesis: Finding sparse, trainable neural networks. *arXiv preprint arXiv:1803.03635*.

Gholami, A.; Kim, S.; Dong, Z.; Yao, Z.; Mahoney, M. W.; and Keutzer, K. 2022. A survey of quantization methods for efficient neural network inference. In *Low-Power Computer Vision*, 291–326. Chapman and Hall/CRC.

Guo, C.; Qiu, Y.; Leng, J.; Gao, X.; Zhang, C.; Liu, Y.; Yang, F.; Zhu, Y.; and Guo, M. 2022. Squant: On-the-fly data-free quantization via diagonal hessian approximation. *arXiv preprint arXiv:2202.07471*.

He, K.; Zhang, X.; Ren, S.; and Sun, J. 2016. Deep residual learning for image recognition. In *Proceedings of the IEEE conference on computer vision and pattern recognition*, 770–778.

Heo, B.; Kim, J.; Yun, S.; Park, H.; Kwak, N.; and Choi, J. Y. 2019. A comprehensive overhaul of feature distillation. In *Proceedings of the IEEE/CVF international conference on computer vision*, 1921–1930.

Hinton, G. 2015. Distilling the Knowledge in a Neural Network. *arXiv preprint arXiv:1503.02531*.

Ho, J.; Jain, A.; and Abbeel, P. 2020. Denoising diffusion probabilistic models. *Advances in neural information processing systems*, 33: 6840–6851.

Hong, I.; Jo, Y.; Lee, H.; Ahn, S.; and Park, S. 2025. Advanced knowledge transfer: Refined feature distillation for zero-shot quantization in edge computing. In *Proceedings of the 40th ACM/SIGAPP Symposium on Applied Computing*, 687–694.

Hubara, I.; Courbariaux, M.; Soudry, D.; El-Yaniv, R.; and Bengio, Y. 2018. Quantized neural networks: Training neural networks with low precision weights and activations. *Journal of Machine Learning Research*, 18(187): 1–30.

Jeon, Y.; Lee, C.; and Kim, H.-y. 2023. Genie: show me the data for quantization. In *Proceedings of the IEEE/CVF Conference on Computer Vision and Pattern Recognition*, 12064–12073.

Kim, M.; Kim, J.; and Kang, U. 2025. SynQ: Accurate Zero-shot Quantization by Synthesis-aware Fine-tuning. In *The Thirteenth International Conference on Learning Representations*.

Krizhevsky, A.; Hinton, G.; et al. 2009. Learning multiple layers of features from tiny images.

LeCun, Y.; Denker, J.; and Solla, S. 1989. Optimal brain damage. *Advances in neural information processing systems*, 2.

Li, Y.; Gong, R.; Tan, X.; Yang, Y.; Hu, P.; Zhang, Q.; Yu, F.; Wang, W.; and Gu, S. 2021. Brecq: Pushing the limit

of post-training quantization by block reconstruction. *arXiv preprint arXiv:2102.05426*.

Li, Y.; Kim, Y.; Lee, D.; Kundu, S.; and Panda, P. 2024. GenQ: Quantization in Low Data Regimes with Generative Synthetic Data. In *European Conference on Computer Vision*, 216–235. Springer.

Liu, Z.; Sun, M.; Zhou, T.; Huang, G.; and Darrell, T. 2018. Rethinking the value of network pruning. *arXiv preprint arXiv:1810.05270*.

Nagel, M.; Baalen, M. v.; Blankevoort, T.; and Welling, M. 2019. Data-free quantization through weight equalization and bias correction. In *Proceedings of the IEEE/CVF International Conference on Computer Vision*, 1325–1334.

Nagel, M.; Fournarakis, M.; Amjad, R. A.; Bondarenko, Y.; Van Baalen, M.; and Blankevoort, T. 2021. A white paper on neural network quantization. *arXiv preprint arXiv:2106.08295*.

Odena, A.; Olah, C.; and Shlens, J. 2017. Conditional image synthesis with auxiliary classifier gans. In *International conference on machine learning*, 2642–2651. PMLR.

Qian, B.; Wang, Y.; Hong, R.; and Wang, M. 2023. Adaptive data-free quantization. In *Proceedings of the IEEE/CVF Conference on Computer Vision and Pattern Recognition*, 7960–7968.

Ruder, S. 2016. An overview of gradient descent optimization algorithms. *arXiv preprint arXiv:1609.04747*.

Sandler, M.; Howard, A.; Zhu, M.; Zhmoginov, A.; and Chen, L.-C. 2018. Mobilenetv2: Inverted residuals and linear bottlenecks. In *Proceedings of the IEEE conference on computer vision and pattern recognition*, 4510–4520.

Wang, L.; and Yoon, K.-J. 2021. Knowledge distillation and student-teacher learning for visual intelligence: A review and new outlooks. *IEEE transactions on pattern analysis and machine intelligence*, 44(6): 3048–3068.

Xu, K.; Li, Z.; Wang, S.; and Zhang, X. 2024. Ptmq: Post-training multi-bit quantization of neural networks. In *Proceedings of the AAAI Conference on Artificial Intelligence*, volume 38, 16193–16201.

Xu, S.; Li, H.; Zhuang, B.; Liu, J.; Cao, J.; Liang, C.; and Tan, M. 2020. Generative low-bitwidth data free quantization. In *Computer Vision–ECCV 2020: 16th European Conference, Glasgow, UK, August 23–28, 2020, Proceedings, Part XII 16*, 1–17. Springer.

Yin, P.; Lyu, J.; Zhang, S.; Osher, S.; Qi, Y.; and Xin, J. 2019. Understanding straight-through estimator in training activation quantized neural nets. *arXiv preprint arXiv:1903.05662*.

Yvinec, E.; Dapogny, A.; Cord, M.; and Bailly, K. 2023. Spiq: Data-free per-channel static input quantization. In *Proceedings of the IEEE/CVF Winter Conference on Applications of Computer Vision*, 3869–3878.

Zoph, B. 2016. Neural architecture search with reinforcement learning. *arXiv preprint arXiv:1611.01578*.

Appendix

Notation

We provide an overview of the main symbols and definitions used throughout the paper, along with their precise mathematical formulations.

Symbol	Definition
A	Original activation tensor
\vec{A}_q	Quantized activation vector (per channel)
\vec{A}	Pre-scaled activation
$\vec{A}_{\min}, \vec{A}_{\max}$	Per-channel min and max activation values
\vec{s}	Per-channel scaling factor vector
\vec{z}	Per-channel zero-point vector
b	Number of quantization bits
C, H, W	Channel, Height, Width dimensions of activation
$\mathbb{R}^{C \times H \times W}$	Activation tensor space
$\lfloor \cdot \rfloor$	Rounding function
\cdot	Element-wise multiplication
$\sum_{c=1}^C$	Channel-wise summation
w_c	Weight for channel c
y_l	Output after accumulation at layer l
Mathematical Expressions	
Scaling Factor	$\vec{s} = \frac{\vec{A}_{\max} - \vec{A}_{\min}}{2^b - 1}$
Zero-point	$\vec{z} = \left\lfloor \frac{-\vec{A}_{\min}}{\vec{s}} \right\rfloor$
Forward Quantization	$\vec{A}_q = \lfloor \frac{A}{\vec{s}} + \vec{z} \rfloor$
Pre-scaled Dequantization	$\vec{A} = \vec{s} \cdot (\vec{A}_q - \vec{z})$
Output Accumulation	$y = \sum_{c=1}^C w_c \cdot \vec{A}_c$
Cosine Similarity	$\frac{X \cdot Q}{\ X\ _2 \ Q\ _2}$
Relative Error	$\frac{\ X - Q\ _2}{\ X\ _2}$

Table 6: Notation and expressions for vectorized channel-wise activation quantization with pre-scaling.

Details of Experimental Setup

We describe the datasets, experimental setup, and baselines to ensure reproducibility and highlight both the effectiveness and implementation accessibility of our approach.

Datasets This paper outlines the experimental settings for CIFAR-10 (Krizhevsky, Hinton et al. 2009), CIFAR-100 (Krizhevsky, Hinton et al. 2009), and ImageNet (ILSVRC-2012) (Deng et al. 2009) datasets. CIFAR-10 and CIFAR-100 contain 10 and 100 classes, respectively, with 32×32 resolution color images, and both have 50 K training and 10 K test images. ImageNet comprises 1,000 classes, with 1.2 M training and 50 K validation images, all resized to 224×224 for our experiments. We employ these widely used benchmarks for zero-shot quantization (ZSQ) to assess and compare the performance of *GranQ* against those of existing approaches.

Experimental Setup The data generation process followed the settings of AdaDFQ (Qian et al. 2023). Specifically, ACGAN (Odena, Olah, and Shlens 2017) was used for data generation with the Adam optimizer, set with a momentum of 0.9 and a learning rate of 1e-3. All hyper-parameters such as α_{ds} , α_{as} , λ_l , and λ_u followed the default settings from AdaDFQ (Qian et al. 2023). For the fine-tuning process, a warmup phase was applied to ensure training stability, with 4 epochs out of 200 for CIFAR and 50 epochs out of 400 for ImageNet. The batch size was set to 16 for CIFAR-10 and ImageNet, and 200 for CIFAR-100. All experiments used Nesterov-based SGD (Nesterov 1983) as the optimizer, with momentum 0.9 and weight decay 1e-4. In CIFAR experiments, the weight decay of 1e-4 was reduced by a factor of 0.1 every 100 epochs, whereas for ImageNet, decay was applied at 350 and 400 epochs (for ResNet-50 at 150, 300, and 400 epochs). *GranQ* was implemented using PyTorch (Paszke et al. 2019), and visualizations were generated with matplotlib (Hunter 2007). All experiments were conducted on an NVIDIA RTX 3090 GPU.

Comparison Methods *GranQ* is a quantization-aware training (QAT) method for zero-shot quantization (ZSQ). Therefore, to evaluate the proposed approach, we conducted comparative experiments using the following state-of-the-art methods:

- **GDFQ (Xu et al. 2020):** GDFQ (Generative low-bit data-free quantization) is the first approach to train quantized models using synthetic data through knowledge distillation. It demonstrated that effective quantization is possible even without access to original data.
- **AIT (Choi et al. 2022):** AIT was the first to show the negative impact of cross-entropy loss when training quantized models with distillation. It also provided a systematic analysis of training strategies in the ZSQ domain.
- **AdaDFQ (Qian et al. 2023):** AdaDFQ (Adaptive data-free quantization) highlighted the generalization issues of generated data under various quantization settings and proposed a more adaptable data generation method.
- **TexQ (Chen et al. 2023):** TexQ introduced a data generation method that preserves texture distributions, thereby enhancing the quality of generated data in ZSQ environments.
- **RIS (Bai et al. 2024):** RIS (Robustness-guided image synthesis) addressed the low semantic quality of generated data and proposed using perturbations to improve data diversity.
- **GenQ (Li et al. 2024):** GenQ introduced the use of stable diffusion in ZSQ, enabling the generation of high-resolution, realistic data.
- **AKT (Hong et al. 2024):** AKT (Advanced knowledge transfer) proposed refining feature information during distillation to improve the training of quantized models.
- **SynQ (Kim, Kim, and Kang 2025):** SynQ enhanced the training of quantized models by reducing noise in generated data using low-pass filtering and aligning activation maps.

Algorithm 2: Conventional Channel-Wise Quantization (Scalar-loop for scaling)

Require: Activation tensors $\{A_l\}_{l=1}^L$, where $A_l \in \mathbb{R}^{C \times H \times W}$, quantization bit b , weights $\{W_l\}_{l=1}^L$

Ensure: Output vectors $\{y_l\}_{l=1}^L$

- 1: **for** each layer l in L **do**
- 2: $A_l \leftarrow \text{reshape}(A_l) \in \mathbb{R}^{C \times (HW)}$
- 3: **for** each channel c in C **do**
- 4: $s_c = \frac{\max(A_{l,c}) - \min(A_{l,c})}{2^b - 1}$
- 5: $z_c = \left\lfloor -\frac{\min(A_{l,c})}{s_c} \right\rfloor$
- 6: $A_{q,l}[c, :] = \left\lfloor \frac{A_l[c, :] - z_c}{s_c} + z_c \right\rfloor$
- 7: **end for**
- 8: **Compute output:**

$$y_l = \sum_{c=1}^C w_{l,c} \cdot (s_c \cdot (A_{q,l}[c, :] - z_c))$$

- 9: **end for**
- 10: **return** $\{y_l\}_{l=1}^L$

Algorithm

While prior works apply vectorized computation only to the quantization step, they compute per-channel scaling parameters through iterative operations. *GranQ* also vectorizes this scaling step, enabling fully parallel quantization. Algorithm 1 summarizes the process with pre-scaling.

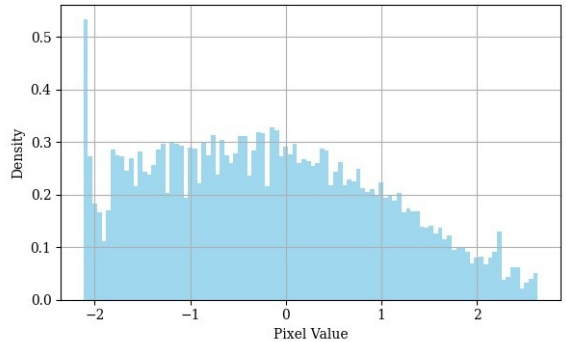
In Algorithm 1, the entire quantization procedure is implemented using vectorized tensor operations across all channels, enabling efficient accumulation without runtime scaling. Specifically, the per-channel minimum and maximum values are computed in parallel, and the corresponding scaling factors and zero-points are applied via broadcasting. This removes the need for channel-wise loops and enables efficient accumulation without runtime scaling, making the procedure highly suitable for modern hardware accelerators.

In contrast, Algorithm 2 adopts a conventional channel-wise quantization scheme, where scaling parameters are computed iteratively for each channel using a for-loop. Although the quantization and dequantization steps are applied in a vectorized manner per channel, the overall process remains sequential due to scalar-based scaling. This incurs significant computational overhead, particularly in networks with a large number of channels.

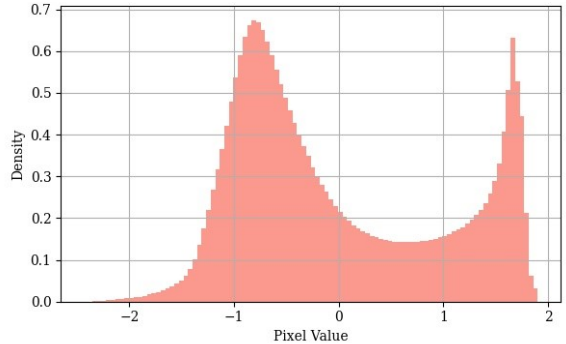
By removing this bottleneck, *GranQ* achieves both higher parallelism and lower latency, which are particularly beneficial in low-bitwidth quantization scenarios.

Extra Analysis

Data Distribution Analysis Figure 5 compares the pixel distributions of original and synthetic inputs derived from ImageNet. The skewness of the original input is 0.2599, whereas that of the synthetic input increases to 0.4877, with the distribution shifted toward higher pixel values. This indicates that synthetic data, often generated without real image



(a) Original inputs (Skewness: 0.2599)



(b) Synthetic inputs (Skewness: 0.4877)

Figure 5: Pixel distribution comparison between (a) original and (b) synthetic inputs on ImageNet. Synthetic inputs generated by AdaDFQ (Qian et al. 2023) exhibit a rightward shift with higher skewness, indicating more extreme activations and highlighting the need for granular scaling.

priors, tends to contain a greater number of extreme activation values. As a result, the likelihood of outliers increases, which fixed-range quantization cannot effectively handle. In particular, when a single global range is applied across all channels, the presence of outliers can compress the majority of values into a narrow dynamic range, leading to severe quantization distortion. These observations underscore the limitations of conventional scaling strategies.

Analysis of Activation Preservation We analyzed how activation distortion propagates across layers in a ZSQ setting where synthetic data is used as input. When coarse quantization is applied without sufficiently granular scaling, distortion tends to accumulate in specific layers and ultimately degrades the output layer’s activation representation. This suggests that insufficient preservation of intermediate activations can negatively affect the quality of final inference. The problem becomes more severe in zero-shot scenarios due to the distributional mismatch introduced by synthetic data. In contrast, *GranQ* mitigates this issue by applying fine-grained channel-wise scaling, resulting in consistently stable activation distributions throughout the network. This phenomenon is clearly demonstrated in Figure 6, where *GranQ* maintains stable activations with noticeably reduced distortion compared to conventional quantization methods.

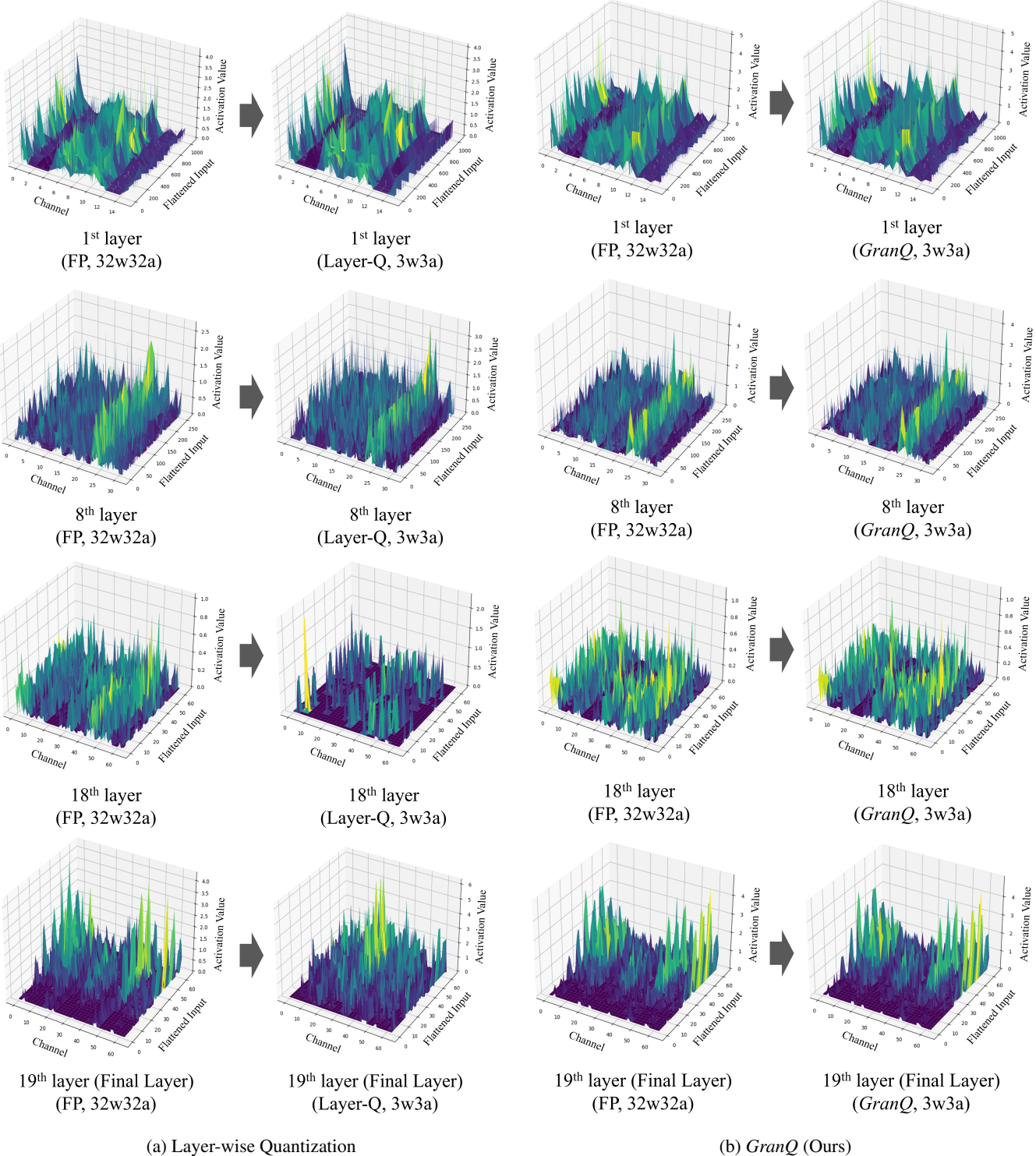


Figure 6: Visualization of activation magnitudes across layers in ResNet-20. (a) illustrates the activation magnitudes with layer-wise quantization, whereas (b) presents the results after applying the proposed *GranQ* method. In each subplot, the left side depicts activation magnitudes before quantization (32-bit), whereas the right side shows them after quantization (3-bit). The proposed *GranQ* effectively preserves the activation distribution, mitigating distortions caused by quantization.

References

Bai, J.; Yang, Y.; Chu, H.; Wang, H.; Liu, Z.; Chen, R.; He, X.; Mu, L.; Cai, C.; and Hu, H. 2024. Robustness-guided image synthesis for data-free quantization. In *Proceedings of the AAAI Conference on Artificial Intelligence*, volume 38, 10971–10979.

Chen, X.; Wang, Y.; Yan, R.; Liu, Y.; Guan, T.; and He, Y. 2023. Texq: zero-shot network quantization with texture feature distribution calibration. *Advances in Neural Information Processing Systems*, 36: 274–287.

Choi, K.; Lee, H. Y.; Hong, D.; Yu, J.; Park, N.; Kim, Y.; and Lee, J. 2022. It’s all in the teacher: Zero-shot quantization brought closer to the teacher. In *Proceedings of the IEEE/CVF Conference on Computer Vision and Pattern Recognition*, 8311–8321.

Deng, J.; Dong, W.; Socher, R.; Li, L.-J.; Li, K.; and Fei-Fei, L. 2009. Imagenet: A large-scale hierarchical image database. In *2009 IEEE conference on computer vision and pattern recognition*, 248–255. Ieee.

Fan, C.; Wang, Z.; Guo, D.; and Wang, M. 2024. Data-free quantization via pseudo-label filtering. In *Proceedings of the IEEE/CVF Conference on Computer Vision and Pattern Recognition*, 5589–5598.

Hong, I.; Jo, Y.; Lee, H.; Ahn, S.; and Park, S. 2024. Advanced Knowledge Transfer: Refined Feature Distillation for Zero-Shot Quantization in Edge Computing. *arXiv preprint arXiv:2412.19125*.

Hunter, J. D. 2007. Matplotlib: A 2D graphics environment. *Computing in science & engineering*, 9(03): 90–95.

Kim, M.; Kim, J.; and Kang, U. 2025. SynQ: Accurate Zero-shot Quantization by Synthesis-aware Fine-tuning. In *The Thirteenth International Conference on Learning Representations*.

Krizhevsky, A.; Hinton, G.; et al. 2009. Learning multiple layers of features from tiny images.

Li, Y.; Kim, Y.; Lee, D.; Kundu, S.; and Panda, P. 2024. GenQ: Quantization in Low Data Regimes with Generative Synthetic Data. In *European Conference on Computer Vision*, 216–235. Springer.

Nesterov, Y. 1983. A method for solving the convex programming problem with convergence rate $O(1/k^2)$. In *Dokl akad nauk Sssr*, volume 269, 543.

Odena, A.; Olah, C.; and Shlens, J. 2017. Conditional image synthesis with auxiliary classifier gans. In *International conference on machine learning*, 2642–2651. PMLR.

Paszke, A.; Gross, S.; Massa, F.; Lerer, A.; Bradbury, J.; Chanan, G.; Killeen, T.; Lin, Z.; Gimelshein, N.; Antiga, L.; et al. 2019. Pytorch: An imperative style, high-performance deep learning library. *Advances in neural information processing systems*, 32.

Qian, B.; Wang, Y.; Hong, R.; and Wang, M. 2023. Adaptive data-free quantization. In *Proceedings of the IEEE/CVF Conference on Computer Vision and Pattern Recognition*, 7960–7968.

Xu, S.; Li, H.; Zhuang, B.; Liu, J.; Cao, J.; Liang, C.; and Tan, M. 2020. Generative low-bitwidth data free quantization. In *Computer Vision–ECCV 2020: 16th European Conference, Glasgow, UK, August 23–28, 2020, Proceedings, Part XII 16*, 1–17. Springer.